Anal Bioanal Chem (2007) 389:527–532
DOI 10.1007/s00216-007-1478-6

ORIGINAL PAPER

Room temperature ionic liquid doped DNA network immobilized horseradish peroxidase biosensor for amperometric determination of hydrogen peroxide

Cunlan Guo · Yonghai Song · Hui Wei · Peicai Li · Li Wang · Lanlan Sun · Yujing Sun · Zhuang Li

Received: 17 May 2007 / Revised: 25 June 2007 / Accepted: 27 June 2007 / Published online: 21 July 2007

Abstract A novel electrochemical H_2O_2 biosensor was constructed by embedding horseradish peroxide (HRP) in a 1-butyl-3-methylimidazolium tetrafluoroborate doped DNA network casting on a gold electrode. The HRP entrapped in the composite system displayed good electrocatalytic response to the reduction of H_2O_2. The composite system could provide both a biocompatible microenvironment for enzymes to keep their good bioactivity and an effective pathway of electron transfer between the redox center of enzymes, H_2O_2 and the electrode surface. Voltammetric and time-based amperometric techniques were applied to characterize the properties of the biosensor. The effects of pH and potential on the amperometric response to H_2O_2 were studied. The biosensor can achieve 95% of the steady-state current within 2 s response to H_2O_2. The detection limit of the biosensor was 3.5 μM, and linear range was from 0.01 to 7.4 mM. Moreover, the biosensor exhibited good sensitivity and stability. The film can also be readily used as an immobilization matrix to entrap other enzymes to prepare other similar biosensors.

Keywords DNA · Room temperature ionic liquid · Horseradish peroxidase · Hydrogen peroxide · Biosensor

C. Guo · Y. Song · H. Wei · P. Li · L. Wang · L. Sun · Y. Sun · Z. Li (✉)
State Key Laboratory of Electroanalytical Chemistry,
Graduate School of the Chinese Academy of Sciences,
Changchun Institute of Applied Chemistry,
Chinese Academy of Sciences,
Changchun, Jilin 130022, China
e-mail: zligroup@yahoo.com.cn

Introduction

Electrochemical sensors have been a diverse and active research field in the last two decades [1]. Especially, enzyme-based electrochemical biosensors have high sensitivity and selectivity of amperometric signal transduction because they relate to the specificity of an enzyme reaction [2–4]. Research into them can help to construct models for study of the mechanism of electron exchange between enzymes in organisms. Moreover, because of their inherent advantages, such as simplicity, low expense, high selectivity and sensitivity [5], enzyme-based electrochemical biosensors have a wide range of potential applications for clinical diagnosis, the food industry, environmental analysis and bioassay [6–9].

Electrochemical biosensors are based on redox behavior of enzymes immobilized on the electrode surface [10]. The immobilization of enzymes to the bare electrode is significant for the performance of biosensors which can provide a pathway for electron transfer between enzymes and the electrode surface [2], and simultaneously supply a microenvironment to retain the biological activity of the enzymes in their native state. To achieve these objectives, a variety of materials, such as lipids [11], biopolymer chitosans [12], functionalized nanomaterials [13] and DNA molecules [14, 15], have been employed as a matrix to connect enzyme molecules with the electrode surface. DNA with a specific double-helix structure may be employed as a kind of ideal material to modify the electrode surface as a matrix, which can afford both biocompatible microenvironments around enzymes entrapped in the membranes and an effective pathway for electron transfer, since the DNA stacked base pairs can be considered as a system of connected π electrons to transfer electrons [16]. Our previous results have demonstrated that a biosensor

based on horseradish peroxidase (HRP) immobilized in DNA films has a good performance [15]. However, the short electron migration within the DNA duplex (about 4 nm) [16] inhibited electron transfer of a larger number of HRP molecules doped in the multi-DNA films.

Room-temperature ionic liquids (RTIL) are organic molten salts that are composed of organic cations and inorganic anions. When the temperature is around room temperature, they are liquids. Owing to their unique chemical and physical properties, such as negligible low vapor pressure, air and moisture stability, high viscosity, good solubility, relatively wide potential window and high conductivity, RTIL have been applied extensively in synthesis, catalysis, separation, biocatalysis, electrochemistry and so forth [17–22]. When RTIL are doped in DNA, DNA ionic liquids may form on some regions of DNA chains, and some compounds like transparent flexible DNA films with high ion conductivity are obtained because of the characteristics of both an ionic liquid and double-strand DNA, which open a new field for the use of DNA as a biomass [23–25]. Furthermore, RTIL have been shown to be proper media in biocatalysis processing as a pure solvent and a cosolvent in aqueous systems or a biphasic system. In these systems, most enzymes have shown higher selectivity, faster rate and greater enzyme stability [26–31].

In the present work, we describe a novel H_2O_2 biosensor by constructing a composite system based on entrapping HRP in a 1-butyl-3-methylimidazolium tetrafluoroborate (BMIM·BF_4) doped DNA network casting on a gold electrode. As a hydrophilic RTIL, BMIM·BF_4 can mix well with DNA. BMIM·BF_4 entrapped in the three-dimensional DNA network can serve as an ionic conductor owing to its good inherent conductivity to provide a pathway to facilitate the electron transfer between HRP, H_2O_2 and the underlying gold electrode. Meanwhile, the BMIM·BF_4 doped DNA network can provide a favorable microenvironment for the protein HRP to retain its native construction and its bioactivity well. The preparation of the biosensor is simply accomplished by directly casting HRP–DNA–BMIM·BF_4 mixtures on a gold electrode. Electrocatalysis of HRP to the reduction of H_2O_2 was demonstrated at the HRP–DNA–BMIM·BF_4 composite film modified gold electrode. In addition, the optimized conditions and the analytical performance of the resulting biosensor were evaluated in detail.

Experimental

Reagents

HRP (EC 1.11.1.7, type X, 250 U mg^{-1}) and pBR322 DNA were purchased from Sino-American Biotechnology (Beijing, China). BMIM·BF_4, (purity greater than 98%) was obtained from Solvent Innovation (Germany). All other chemicals, including 30% H_2O_2 solution, were purchased from Beijing Chemical Reagent Factory (Beijing, China). All agents were of analytical grade and were used as received. Phosphate-buffered solutions (PBS) were obtained by mixing aqueous solutions of 0.2 M NaH_2PO_4 and 0.2 M Na_2HPO_4 and the pH values were adjusted with 0.1 M H_3PO_4 or NaOH. Fresh H_2O_2 solution was prepared freshly daily with 0.2 M PBS (pH 6.5). All solutions were prepared using ultrapure water (resistivity greater than 18.2 MΩ cm) sterilized at high temperature.

Apparatus

Optical spectra was obtained with a Cary-500 UV–vis–near IR spectrometer (Varian USA) using a transparent glass substrate.

Cyclic voltammetry was carried out and amperometric *i–t* curves were obtained with a CHI 660A electrochemistry workstation (Shanghai, China). All electrochemistry experiments were performed with a homemade three-electrode cell using the enzyme electrode as the working electrode, an Ag/AgCl (saturated KCl) as the reference electrode and a platinum wire as the counter electrode. All potentials reported in this work referred to this reference electrode. All electrochemical measurements were carried out in N_2-purged 0.2 M PBS as the supporting electrolyte at room temperature. Amperometric experiments were accomplished in stirring solutions.

Preparation of film electrode

Before modification, a gold electrode (diameter 3 mm) was first polished with alumina slurry (followed by 1.0, 0.3 and 0.05 μm) and ultrasonically cleaned with double-distilled water and dried in nitrogen. To prepare the HRP–DNA–BMIM·BF_4/gold electrode, a 10-μL mixture of HRP (PBS pH 6.5), DNA (50 ng μL^{-1}) and BMIM·BF_4 was cast onto the gold electrode surface and air-dried at 4 °C in a refrigerator. The electrode prepared was maintained under the same condition when not in use or was measured at 25 °C.

Spectroscopic analysis

Thin glass slides were used as spectroscopic analysis substrates and were cleaned by ultrasonication sequentially in a soap solution and a saturated sodium hydroxide mixed solution (1:1 mixture of water and ethanol) for 20 min respectively. The slides were flushed with double-distilled water after each ultrasonication cleaning. The cleaned slides were dried in nitrogen. Sample films for visible absorption

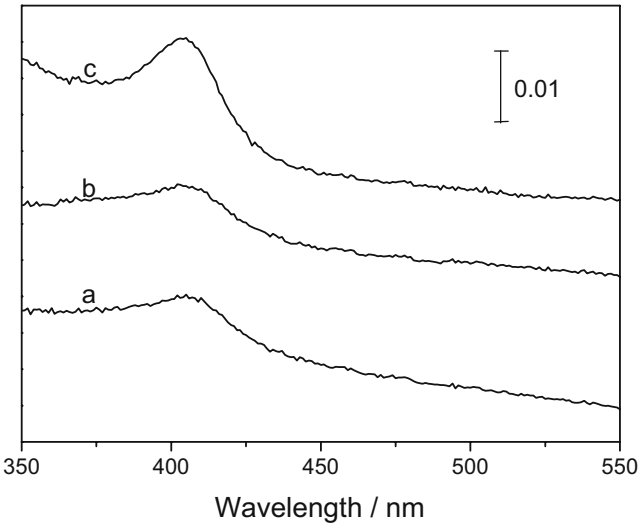

Fig. 1 UV–vis spectra of dry horseradish peroxidase (HRP) film (a), dry HRP–DNA film (b) and the dry HRP–DNA–1-butyl-3-methylimidazolium tetrafluoroborate (BMIM·BF_4) film (c) on thin transparent glass slides at room temperature

spectroscopic measurement were prepared by spreading 10 μL of sample solutions (HRP solution, HRP–DNA solution or HRP–DNA–BMIM·BF_4 solution) onto the cleaned glass slides. The modified slides were then stored at 4 °C in a refrigerator for overnight drying and were measured at 25 °C. A similar glass slide was used as a background.

Results and discussion

UV–vis absorption spectroscopy characterization

UV–vis absorption spectroscopy can provide information on the secondary structure of proteins. The Soret absorption (π–π* transition located mainly on porphyrin) of heme proteins reports mainly on the change in the spin state of the heme iron owing to changes in its axial ligands and gives important information on the conformational change around the region of the heme cavity [32]. Figure 1 shows the UV–vis absorption of different dry films. The dry film of HRP had a Soret band centered at 404 nm (Fig. 1, curve a), which is in agreement with the heme band at 404 nm for native HRP in phosphate buffer (pH 6.0) [33]. The Soret absorption bands of the HRP–DNA film and the HRP–DNA–BMIM·BF_4 film were centered at 403 nm (Fig. 1, curve b) and 404 nm (Fig. 1, curve c), respectively, and displayed almost no shift from the Soret absorption band of HRP film alone, and BMIM·BF_4 had no absorption in this region of the spectrum (data not shown). All these results show that the secondary structures around the heme iron of HRP embedded in DNA or DNA–BMIM·BF_4 films have no significant effect compared with the HRP film alone, which indicates that HRP in the HRP–DNA–BMIM·BF_4 film can retain its activity center of biological catalysis. The composite system based on a DNA network and BMIM·BF_4 thus has good biocompatibility for HRP.

Electrocatalytical behavior of the modified electrode

The electrocatalytic properties of the HRP–DNA–BMIM·BF_4/gold electrode towards the electrochemical reduction of H_2O_2 were first investigated with cyclic voltammetry in PBS solutions. Figure 2 shows the cyclic voltammograms of the HRP-DNA-BMIM·BF_4 film/gold electrode in 0.2 M PBS (pH 6.5) with different H_2O_2 concentrations. In the absence of H_2O_2, no obvious current was found (Fig. 2, curve a), while when a definite concentration of H_2O_2 was added, a dramatic catalytic current was observed, which indicates the reduction of H_2O_2 (Fig. 2, curve b–e). Figure 2 also shows that the catalytic current increases with increasing concentrations of H_2O_2. This result suggests that the catalytic current of the HRP–DNA–BMIM·BF_4 film/gold electrode depends on the concentration of H_2O_2, and can be used for quantitative determination of the concentrations of H_2O_2.

In order to verify whether the current is due to the enzymatic reduction of H_2O_2, a control experiment was performed. Figure 3 shows cyclic voltammograms of differently modified electrodes in the presence of 2.4 mM H_2O_2 solution. The current responses to H_2O_2 on the bare gold electrode and the DNA–BMIM·BF_4/gold electrode were both weak though the response of the DNA–BMIM·BF_4/gold electrode was a little bigger than that of the bare gold electrode (Fig. 3, curves a and b). The

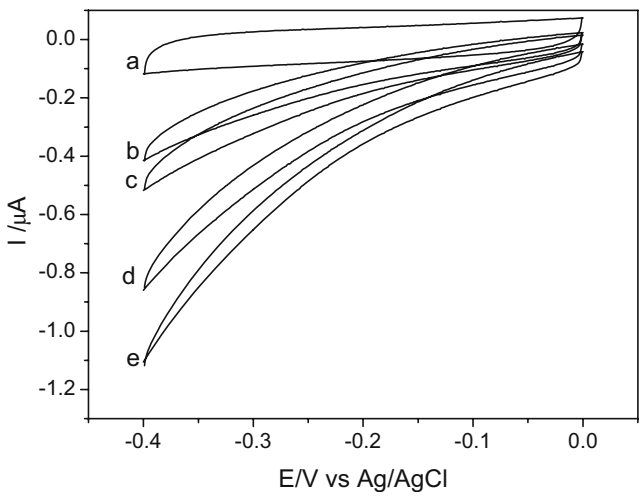

Fig. 2 Cyclic voltammograms of the HRP–DNA–BMIM·BF_4/gold electrode in 0.2 M phosphate-buffered saline (PBS; pH 6.5) with different H_2O_2 concentrations: a 0 mM; b 0.6 mM; c 0.8 mM; d 1.6 mM; and e 2.4 mM. Scan rate 10 mV s^{-1}

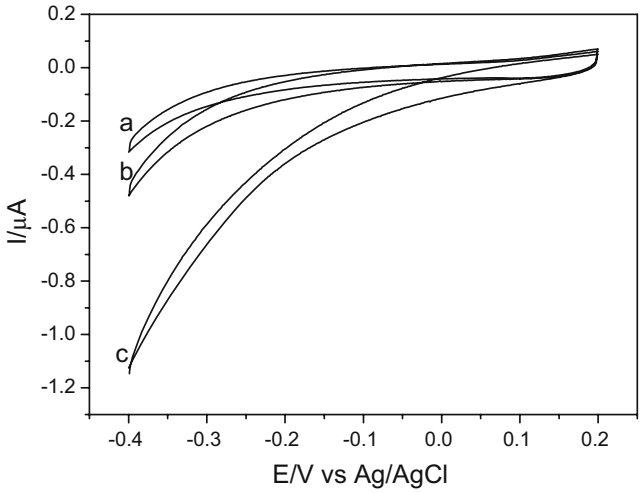

Fig. 3 Cyclic voltammograms of different electrodes in 0.2 M PBS (pH 6.5) with 2.4 mM H_2O_2: a bare gold electrode; b DNA–BMIM·BF_4/gold electrode; and c HRP–DNA–BMIM·BF_4/gold electrode. Scan rate 10 mV s^{-1}

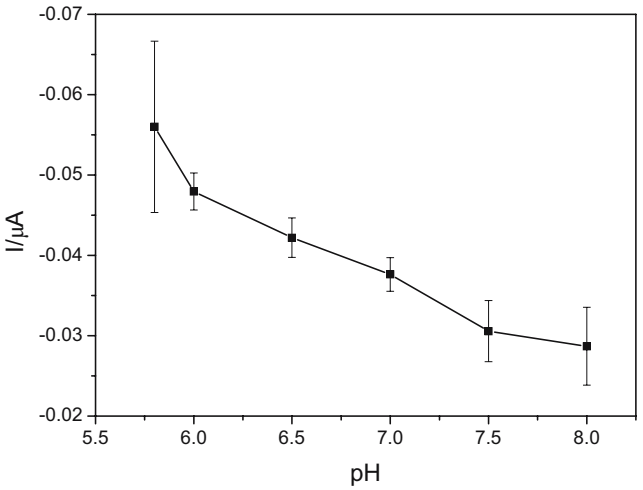

Fig. 5 Effect of pH on the amperometric responses in the presence of 1 mM H_2O_2 in 0.2 M PBS. Applied potential −0.250 V

catalytic current at both these electrodes was small compared with that at the HRP–DNA–BMIM·BF_4/gold electrode (Fig. 3, curve c). These results suggest that H_2O_2 is mainly reduced by HRP entrapped in the DNA–BMIM·BF_4 film. It indicates that HRP in the mixed films may keep its catalytic activity well, and simultaneously exchange electrons with both H_2O_2 and electrode surface. Furthermore, it may predict that the film shows good biocompatibility and provides a favorable microenvironment for HRP to preserve the native structure and exchange electrons with the electrode. These suggestions are consistent with the results described above.

Optimization of experimental variables

The effect of the applied potential on the steady-state current and the pH of the supporting electrolyte are the two major factors that influence the performance of the H_2O_2 sensor. Figure 4 shows the effect of the applied potential on the steady-state current of the HRP–DNA–BMIM·BF_4 film/gold electrode in the presence of 1 mM H_2O_2 (0.2 M PBS with pH 6.5). Electroreduction of H_2O_2 can be observed at −0.05 V. As the applied potential shifted negatively from −0.05 V to −0.35 V, the steady-state current increased gradually. This may result from the increased driving force for the fast H_2O_2 reduction at lower potential [3]; therefore, a lower working potential was chosen as the working potential. In this work −0.25 V was used as the working potential for amperometric determination of H_2O_2 in the

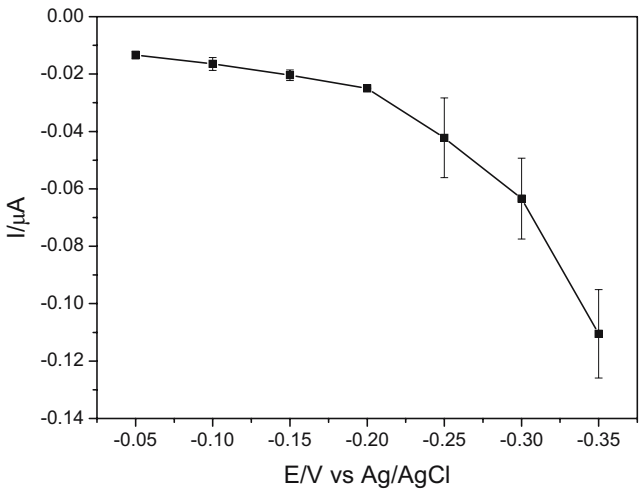

Fig. 4 Effect of applied potential on the amperometric responses in the presence of 1 mM H_2O_2 in 0.2 M PBS (pH 6.5)

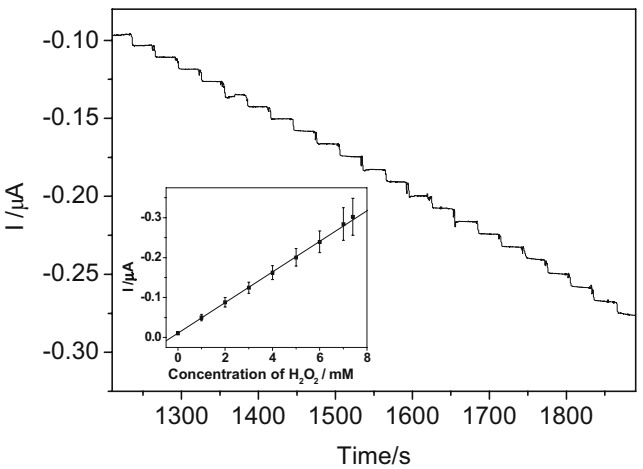

Fig. 6 Typical steady-state response of the biosensor on successive injection of 0.2 mM H_2O_2 into 5 mL stirred PBS. The *inset* shows the calibration curve of current to H_2O_2 concentration. Applied potential −0.250 V, supporting electrolyte 0.2 M PBS (pH 6.5)

following experiments. At −0.25 V, the current responses obtained were sufficient and the background current and noise decreased. Besides that, other potentials could have been used and the final potential could be chosen depending on application of the biosensor, which meant different matrices and different interferences would have different demands.

The effect of pH on the HRP–DNA–BMIM·BF_4 film/gold electrode was also investigated between 5.7 and 8.0 in the presence of 1 mM H_2O_2 in 0.2 M PBS with an applied potential of −0.25 V. Figure 5 shows that the steady-state current decreased as the acidity decreases, which is consistent with our previously reported result [15]. This pH effect can be assigned to the fact that the proton transfer is coupled with the electron transfer in the catalytic reaction [34]. Because many H_2O_2 sensors based on HRP have been investigated and applied in physiological conditions, 0.2 M PBS at pH 6.5 was chosen as the supporting electrolyte in this work.

The current response and calibration curve of the HRP–DNA–BMIM·BF_4 film/gold electrode

Under the aforementioned optimal conditions, a typical current–time curve of the biosensor was recorded by successively adding 0.2 mM H_2O_2 into continuously stirred 0.2 M PBS (pH 6.5). As depicted in Fig. 6, the reduction current rose steeply to reach a stable value, when an aliquot of 0.2 mM H_2O_2 was added to the stirred PBS. The response time to achieve 95% of the steady-state current is within 2 s. Such a fast response can be attributed to the effects as follows. The DNA network may provide a favorable microenvironment for HRP to preserve its native activity; meanwhile, the BMIM·BF_4 entrapped in the DNA network can facilitate electron transfer between HRP and the electrode surface. The inset in Fig. 6 shows the calibration curve of the biosensor for the measurement of H_2O_2. The linear range of the H_2O_2 detection was from 0.01 to 7.4 mM (the correlation coefficient was 0.999, n= 9), and the detection limit was estimated to be 3.5 μM based on the criterion of a signal-to-noise ratio of 3. The performances obtained in our work were not less than those obtained by others [3, 11–14] with other methods of connecting enzymes.

Reproducibility and stability

The reproducibility of the current response of the same modified electrode was examined in 0.2 M PBS (pH 6.5) containing 1 mM H_2O_2. The relative standard deviation was 2.9% for six successive assays. The stability of the modified electrode was also investigated. In a typical experiment, the biosensor was stored in a refrigerator at 4 °C for 2 weeks, and was measured every 2–3 days; no obvious change of current in the response to 1 mM H_2O_2 was found. The good stability was attributed to the BMIM·BF_4 entrapped DNA network that can immobilize the HRP molecules well and provide a biocompatible microenvironment.

Conclusion

A novel electrochemical H_2O_2 biosensor was designed by entrapping HRP in a BMIM·BF_4 doped DNA network casting on a gold electrode. UV–vis absorption spectra showed that HRP molecules kept their native secondary structures around the heme iron of HRP embedded in DNA–BMIM·BF_4 films. The BMIM·BF_4 doped DNA films provided a good biocompatible microenvironment to keep the biological activity of HRP molecules, and a pathway for electron transfer between HRP, H_2O_2 and the solid electrode surface. The biosensor exhibited fast amperometric response (within 2 s), a low detection limit and a broad linear range for H_2O_2. Furthermore, the sensor exhibited good sensitivity and stability. This approach may provide a simple immobilization method in general to prepare biosensors based on enzymes.

Acknowledgement This work was supported by the National Natural Science Foundation of China.

References

1. Bakker E, Qin Y (2006) Anal Chem 78:3965–3984
2. Willner I, Katz E (2000) Angew Chem Int Ed Engl 39:1180–1218
3. Jia JB, Wang BW, Wu AG, Cheng GJ, Li Z, Dong SJ (2002) Anal Chem 74:2217–2223
4. Yu DH, Renedo OD, Blankert B, Sima V, Sandulescu R, Arcos J, Kaufmann JM (2006) Electroanalysis 18:1637–1642
5. Armstrong FA, Heering HA, Hirst J (1997) Chem Soc Rev 26:169–179
6. Wang J, Chen L, Hocevar SB, Ogorevc B (2000) Analyst 125:1431–1434
7. Luo XL, Xu JJ, Du Y, Chen HY (2004) Anal Biochem 334:284–289
8. Bongiovanni C, Ferri T, Poscia A, Varalli M, Santucci R, Desideri A (2001) Bioelectrochemistry 54:17–22
9. Nostu H, Tatsuma T, Fujishima A (2002) J Electroanal Chem 523:86–92
10. Murphy L (2006) Curr Opin Chem Biol 10:177–184
11. Tang JL, Wang BQ, Wu ZY, Han XJ, Dong SJ, Wang EK (2003) Biosens Bioelectron 18:867–872
12. Wang G, Xu JJ, Chen HY, Lu ZH (2003) Biosens Bioelectron 18:335–343
13. Wang L, Wang EK (2004) Electrochem Commun 6:225–229
14. Chen XH, Ruan CM, Kong JL, Deng JQ (2000) Anal Chim Acta 412:89–98

15. Song YH, Wang L, Ren CB, Zhu GY, Li Z (2006) Sens Actuators B 114:1001–1006
16. Holmlin RE, Dandliker PJ, Barton JK (1997) Angew Chem Int Ed Engl 36:2714–2730
17. Welton T (1999) Chem Rev 99:2071–2083
18. Visser AE, Swatloski RP, Rogers RD (2000) Green Chem 2:1–4
19. Wasserscheid P, Welton T (eds) (2002) Ionic liquids in synthesis. Wiley-VCH, Weinheim
20. Anderson JL, Armstrong DW, Wei GT (2006) Anal Chem 78:2892–2902
21. Maleki N, Safavi A, Tajabadi F (2006) Anal Chem 78:3820–3826
22. García-UrdialesE,AlfonsoI,GotorV(2005)ChemRev105:313–354
23. Ohno H, Nishimura N (2001) J Electrochem Soc 148:E168–E170
24. Nishimura N, Ohno H (2002) J Mater Chem 12:2299–2304
25. Nishimura N, Nomura Y, Nakamura N, Ohno H (2005) Biomaterials 26:5558–5563
26. Park S, Kazlauskas RJ (2003) Curr Opin Biotechnol 14:432–437
27. Kim KW, Song B, Choi MY, Kim MJ (2001) Org Lett 3:1507–1509
28. Rantwijk FV, Lau RM, Sheldon RA (2003) Trends Biotechnol 21:131–138
29. Kragl U, Eckstein M, Kaftzik N (2002) Curr Opin Biotechnol 13:565–571
30. Okrasa K, Guibé-Jampel E, Therisod M (2003) Tetrahedron Asymmetry 14:2478–2490
31. Machado MF, Saraiva JM (2005) Biothchnol Lett 27:1233–1239
32. Tang JL, Jiang JG, Song YH, Peng ZQ, Wu ZY, Dong SJ, Wang EK (2002) Chem Phys Lipids 120:119–129
33. Jia NQ, Zhou Q, Liu L, Yan MM, Jiang ZY (2005) J Electroanal Chem 580:213–221
34. Bond AM (ed) (1980) Modern polarographic methods in analytical chemistry. Dekker, New York